What Drives Plate Motion?

Yongfeng Yang
Bureau of Water Resources of Shandong Province, Jinan, China

Abstract

Plate motion was widely thought to be a manifestation of mantle dynamics. However, an in-depth investigation shows this understanding incompetent. Here we propose, the tide-related oceans yield varying pressures between them, the application of these pressures to the continent's sides forms enormously unequal horizontal forces (i.e., the ocean-generating forces), the net effect of these forces provides lateral push to the continent and may cause it to move horizontally, further, the travelling continent works its adjacent crusts to move, these totally form plate motion. A roughly estimation shows that the ocean-generating force may give South American, African, Indian, and Australian continents a movement of respectively 2.8, 4.2, 5.7, and 6.3 cm/yr, and give Pacific Plate a movement of 8.9 cm/yr. Some torque effects of the ocean-generating force contributes to rotate North American and Eurasian continents.

1 Introduction

One of the most significantly achievements in the 20th century was the establishment of the plate tectonics that developed from the earlier conception of continental drift. The continent drift theory hypothesized that the continents had slowly floated over the Earth's surface in the distant past (Wegener, 1915 and 1924). The evidences supporting this surface motion include a shape fitting at the opposed sides of African and American continents, coal belt crossed from North American to Eurasian, identical direction of ice sheet of southern Africa and India, and speed measurement made by global positioning system (GPS). In addition, the discovery of paleomagnetic reversals in oceans, which reflects seafloor spreading, further consolidated the belief of Earth's surface motion (Hess, 1962; Vine and Matthews, 1963). Nevertheless, the driving force behind this motion always remains poorly understood, regardless of unremitting efforts made by geophysicists in the past 100 years. The first to consider the dynamics source of this surface motion is the contraction theory, which proposed that a wrinkling process of Earth's surface had forced the Himalayas to climb up. Wegener (1915) directly ascribed continent's drift to the centrifugal and tidal drag forces, but these forces were latterly found to be too weak to work. For instance, Jeffreys (1929) claimed that the mean tidal friction slowing the Earth's rotation corresponds to a westward stress of the order of only 10^{-4} dyn/cm^2 over the Earth's surface, this stress is too small to maintain the drift. This discrepancy also lead the continental drift theory to be rejected. After these attempts failed, people began to turn their eyes to the interior of the Earth to seek for the answer, together with the rebirth of the continental drift theory in the form of 'plate tectonics', this cultivated a series of various driving forces like basal drag, slab suction, ridge push, slab-pull, tidal drag, the geoid's deformation, the Coriolis force, and the centrifugal force to account for plate motion (Holmes, 1931; Runcorn, 1962a, b; Turcotte and Oxburgh, 1972; Oxburgh and Turcotte, 1978; Spence, 1987; White & McKenzie, 1989; Conrad & Lithgow-Bertelloni, 2002). Among of these driving forces, both basal drag and slab suction relate to mantle dynamics and are thought to be the first level force. Mantle dynamics considers mantle convection currents as the dynamic source of plate motion (Holmes, 1931; Pekeris, 1935; Hales, 1936; Runcorn, 1962a, b;

Turcotte and Oxburgh, 1972; Oxburgh and Turcotte, 1978; Tanimoto & Lay, 2000; Bercovici, et al., 2015). Simply, it provided a basal drag exerted by mantle convective current along the more rigid overlying lithosphere, and a slab suction generated by local mantle convection current exerting a downward pull on plate in subduction zone. Both ridge push and slab-pull relate to gravity and are thought to be the second level force. Ridge push represents a gravitational sliding of the increasingly cooling and thickening plate away from a spreading ridge (Spence, 1987; White & McKenzie, 1989), whereas slab-pull mainly proposes a cold, dense sinking plate uses its weight to pull other plate it attaches to (Conrad & Lithgow-Bertelloni, 2002). The remaining forces relate to the Earth's rotation and are thought to be the systematic force. As the systematic force is almost symmetrical relative to the Earth's shape, it may be easily excluded. Finally, these four forces, i.e., basal drag, slab suction, ridge push, and slab-pull, are left to be the dominant forces to account for plate motion. At first glance, these driving forces are so abundant that they might be competent for plate motion. The fact, however, is not so. Behind them, it shows highly chaotic and unclear. First of all, let's check the applicability of these driving forces. The asthenosphere is insufficiently rigid that it cannot cause motion by basal friction along the base of the lithosphere, slab pull is therefore thought be the greatest force to drive plate motion (Conrad and Lithgow-Bertelloni, 2002). However, most of plates (South American, North American, Eurasian, and Antarctic Plates, for instance) don't hold these features of subducting into trenches. This means that no slab pull may be available for these plates. Ridge push is only applicable for a plate whose one end stands at the spreading center whereas another end is sinking at the subduction zone, it is this slight tilt to provide a gravitational sliding to drive the plate to move. For these two plates like South American and North American, the continent loading at the west of the plate forms a tilt to fight against the tilt that is due to the ridge loading at the east, thus, the ridge push is useless. And then, without slab pull and ridge push, and also due to the weakness of the asthenosphere, one cannot find any effective force to work these plates. Second, let's check the dynamic sources of these driving forces. Both basal drag and slab suction are rooted from the mantle dynamics that is usually depicted with some wheel-like convection currents, however, some techniques based on 3D seismic tomography still cannot recognize these large-scale convection currents. Back to the issue of ridge push and slab-pull, as plates are steadily moving over the Earth's surface, this means a plate may ride over another plate in the front and at the same time depart from a third plate in the rear, it is natural to form a subduction zone and a fracture zone at both ends. The fracture zone, if severe enough to pierce the lithosphere, would allow the magma to erupt, eventually forming the mid-ocean ridge (MOR). From this viewpoint, the subducting plate and the MOR themselves may be a sequence of plate motion. But nowadays, the subducting plate and the MOR are treated as a passage to yield slab-pull and ridge push to further drive themselves. This goes to the chicken-or-egg question, who is the first? In physical field, it is required that a movement (i.e., result) must be separated clearly from the force (i.e., cause) that supports it. Third, the diversity of plate motions greatly challenges these driving forces. Some plates (South American, African, and Indian-Australian, for instance) move approximately along straight path, while others (Eurasian and North American) run in a rotating way. Most strangely, both Indian-Australian and Pacific plates move nearly orthogonal to each other. It is considerably difficult to imagine how these driving forces work together to manage these various surface motions. In the scenarios of the mantle convection theory, poloidal motion involves vertical upwellings and downwellings, while toroidal motion undertakes horizontal rotation (Bercovic, et al., 2015). The generation of torioidal motion requires variable viscosity, but unfortunately, numerous studies of basic 3-D convection with temperature-dependent viscosity had failed to yield the requisite toroidal flow (Bercovic, 1993, 1995b; Cadek et al., 1993; Christensen and Harder, 1991; Stein et al., 2004; Tackley, 1998; Trompert and Hansen, 1998; Weinstein, 1998). Last, these driving forces are unsuccessful in yielding plate motions, although some models had yielded plate-like behavior and mathematically got solution for plate motion velocity by means of a non-Newtonian way, i.e., a balance relationship of buoyancy force and drag force (Bercovici, et al., 2015). Some authors could argue that the global 3-D convection models have successfully shown how mantle density variations can drive convection currents and

plates at the surface. One should be aware, these modelling works address the plates may be moving under the constrain of some ideally conditions, but we cannot exclude that the plates also may be moving under the constrain of other conditions. For example, as demonstrated in the following sections, we have also successfully used another passage to realize plate motion (including speed and direction) that is completely comparable to observation. We feel, to prove that plate motion is really related to the mantle density variations, one has to find direct evidence to support. Besides these shortcomings, other problems like changes in plate motion, plateness, and asymmetry of subduction also remains unresolved within the paradigm of these driving forces (Bercovici, et al., 2015). Since 1970's, some had begun to discuss the relative importance of these driving forces (Forsyth & Uyeda, 1975; Backus, et al., 1981; Bokelmann, 2002). This discussion give people the sense that all the forces related to plate motion had been known well. The fact, however, is not so, another force has been neglected by scientific community. In this work, we go back to the exterior of the Earth to seek this force and consider a solution for plate motion.

2 A tide-related ocean driving mechanism for plate motion

2.1 Ocean-generating force for continent

Liquid can exert pressure at the side of a vessel that holds it. Refer to the top of Figure 1, the total pressure at the side of a cubic vessel may be roughly written as $P=\rho g y/2$, the application of this pressure to the side generates force for this side, which may be expressed as $F=PS=\rho g y^2 x/2$, where S is the area of the side that is applied by the pressure, ρ, g, x, and y are respectively density of liquid, gravitational acceleration, vessel width, and liquid depth. Go back to real world, ocean is a naturally gigantic vessel whose sides consist of continents, and its depth is usually more than thousands of meters, these determine that ocean may generate enormous pressure for the continent's side. Most of oceans experience two cycles of high and low water per day, and the amplitude of this oscillation often reaches a few meters, these are the tides we see in everyday life. Connected to the expression we made above, the addition of the daily tide to ocean generates varying pressure within ocean, and further, the application of this varying pressure to the continent's side generates enormous varying force for the continent. Ocean pressure variations had been extensively found by means of bottom pressure measurements around the globe (Fig. 2). Bottom pressure measurements also reflect a fact that ocean pressure variations not only closely relate to the daily tides but greatly differ from one ocean to another. For example, at the time of new Moon of the month, the range of bottom pressure variation at North Santo Domingo (Atlantic ocean) is almost within 100 millibars, while at South Dutch Harbor (Pacific ocean) this range may reach up to 260 millibars. Ocean pressure always exerts on the continental slope to form normal force, this normal force can be further decomposed into horizontal force and vertical force. We here define the continental crust, which has been applied by ocean pressure, as continent in the following sections. According to Figure 1, the net force of all these forces for the continent may be written as

$$F = (F_L' - F_R') - (f_{base} + f_{right} + f_{left} + f_{far} + f_{near}) \quad (1)$$

where the first term $(F_L' - F_R')$ denotes the total horizontal force, the second term $(f_{base} + f_{right} + f_{left} + f_{far} + f_{near})$ denotes the total resistive force. F_L' and F_R' are the horizontal forces generated at the two sides of the continent and may be further written as $F_L'=0.5\rho g L(h_L+h_L')^2$, $F_R'=0.5\rho g L(h_R+h_R')^2$, and ρ, g, L, h_L, and h_R are respectively density of water, gravitational acceleration, ocean's width (also continent's width), ocean depth at the left, and ocean depth at the right, h_L' and h_R' are respectively the tidal heights at both sides. The tidal heights can be expressed as $h_L'=A_L\sin\omega t$, and $h_R'=A_R\sin(\omega t+\varphi)$, A_L and A_R denote tidal amplitudes, ω, t, and φ are respectively angular frequency, time, and phase difference between the tides at both sides. f_{base} is the friction exerted by the asthenosphere along the continent's base, f_{right}, f_{left}, f_{far},

and f_{near} are respectively the push force from the crust at the right side, the pull from the crust at the left side, the shearing from the crust at the far side, and the shearing from the crust at the near side.

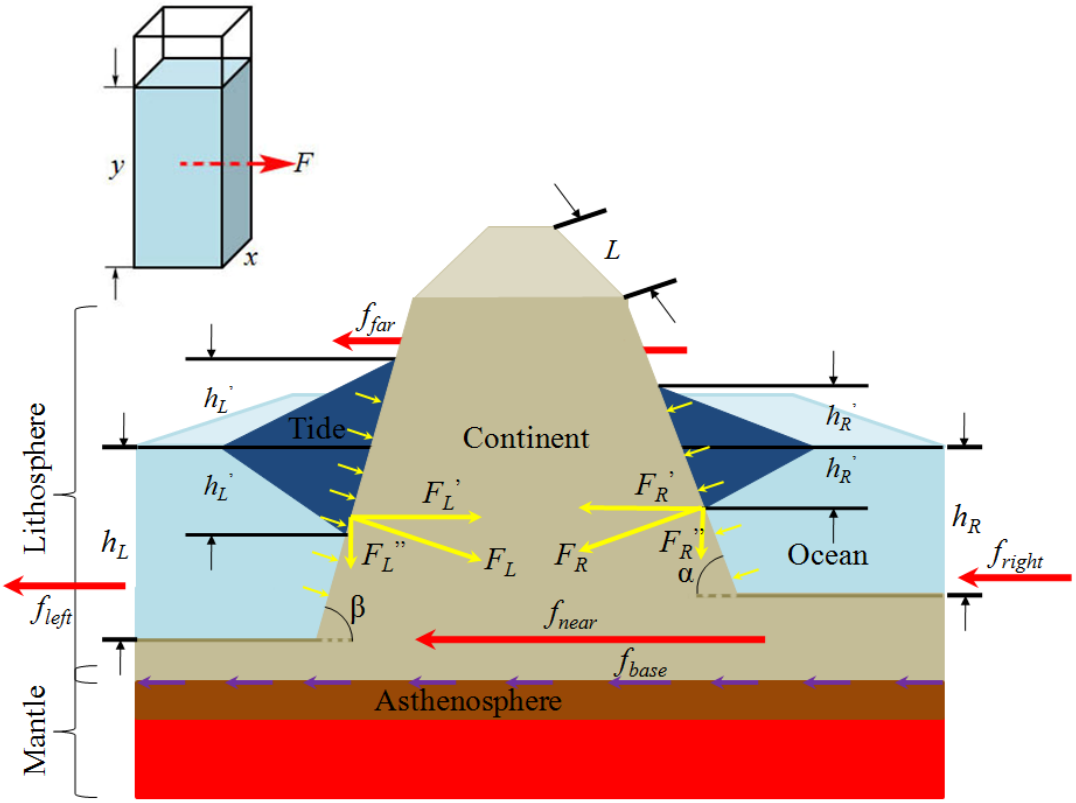

Fig. 1. Modelling the dynamics of the continent under the effect of ocean and tide. $F_L(F_R)$ represents the normal force generated at the left (right) side of the continent, while F_L'(F_R') and F_L''(F_R'') denote respectively the horizontal and vertical forces decomposed from the normal force. f_{base} denotes the friction from the asthenosphere, while f_{right}, f_{left}, f_{far}, and f_{near} denote the push force from the crust at the right side, the pull force from the crust at the left side, the shearing from the crust at the far side, and the shearing from the crust at the near side of the continent. L denotes the width of continent's side, h_L and h_R are respectively ocean depth at the left and at the right, h_L' and h_R' are the tidal heights at both sides. α and β denote the inclinations of the continent's slope at both sides. Note that the tidal heights are highly exaggerated relative to ocean depth.

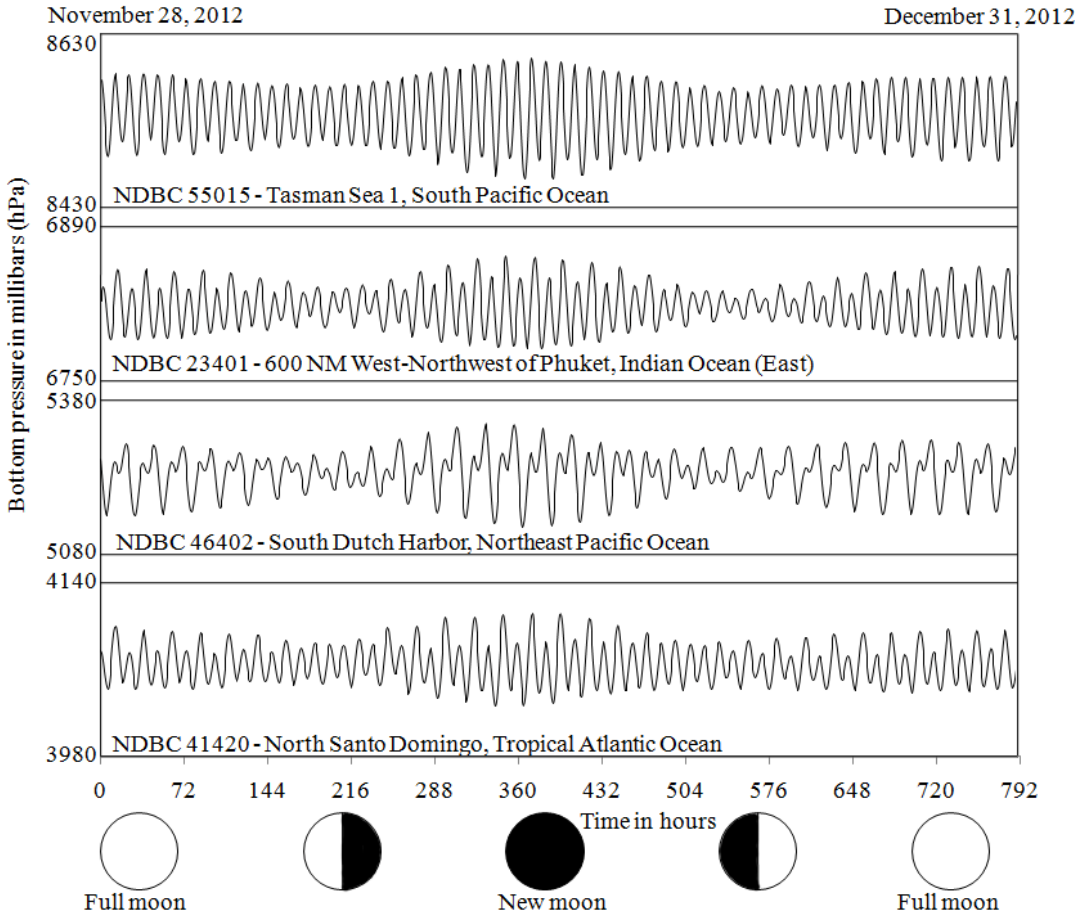

Fig. 2. Typical 1-month bottom pressure records from Pacific, Atlantic, and Indian oceans during 2012. Bottom pressure record data are from PSMSL (Permanent Service for Mean Sea Level).

2.2 Continent's movement

The equation (1) provides three possibilities for the continent. If the total horizontal force is less than or equal to the total resistive force, it represents the total horizontal force cannot overcome the total resistive force, if the total horizontal force is greater than the total resistive force, it represents the total horizontal force can overcome the total resistive force, the continent gets a lasting force, and if the total horizontal force is sometime greater than the total resistive force but sometime less than the total resistive force, it represents the continent gets a discontinuous force. As a lasting force can yield an accelerative movement for an object, it is impossible for the continent to hold such a force. We finally allow the continent to get a discontinuous force. To facilitate the following deduction, we divide the total horizontal force (F_L'- F_R') into two parts: the horizontal force generated due to ocean (marked with F_{ocean}) and the horizontal force generated due to tide (marked with F_{tide}), and further assume the total resistive force (marked with $F_{resistive}$) is fixed and its magnitude is slightly less than the maximum of the total horizontal force. And then, under the effect of a discontinuous force, the continent's movement may be described as below: refer to Figure 3, at the stage of t_1, the total horizontal force begins to increase as the tidal height increases, but since $(F_{ocean}+F_{tide})-F_{resistive}$ <0, the continent remains motionless; At the stage of t_2, $(F_{ocean}+F_{tide})-F_{resistive}$ >0, the continent accelerates to move, and its speed reaches a high level at the end of this period; At the stage of t_3, $(F_{ocean}+F_{tide})-F_{resistive}$ <0, the continent begins to decelerate until its speed reaches zero at the end of this period; At the stage of t_4, due to $(F_{ocean}+F_{tide})-F_{resistive}$ <0, the continent remains motionless; And at the stage of t_5 and t_6, the

continent obtains a movement that is similar to that movement at the stage of t_2 and t_3, but at the stage of t_7, the continent remains motionless again. Simply, the continent discontinuously obtains some movements at the stage of t_2, t_3, t_5, and t_6, and some stagnations at the stage of t_1, t_4, and t_7. This relationship represents a net forward movement for the continent during the day. Expanding this day to the whole year, it indicates that the continent obtains a steadily movement during the year. Further, extending this case to a long-lived ocean and to the fact that the tides are extensively distributed around the globe, we conclude that the continents had obtained steadily movements over millions of years. Figure 4 exhibits a globally distribution of the tides and the horizontal forces generated due to ocean.

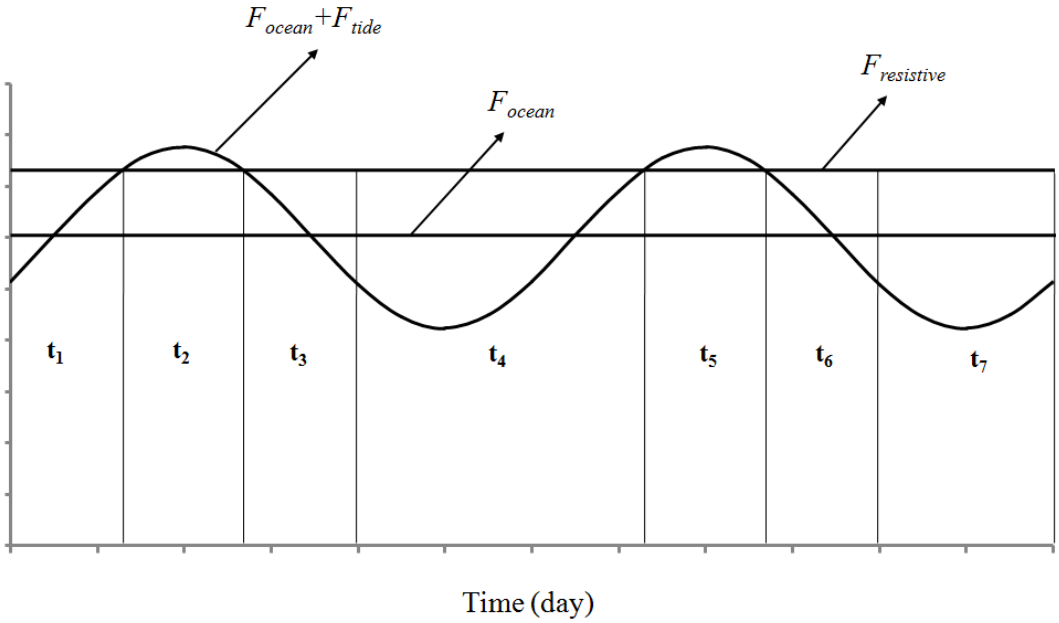

Fig. 3. Dynamic analysis for continent. F_{ocean} and F_{tide} denote respectively the horizontal force generated due to ocean and the horizontal force generated due to tide, $F_{resistive}$ denotes the total resistive force, which consists of the friction exerted by the asthenosphere along the continent's base and the resistive force from adjacent crusts. Note, the oscillation of the total horizontal force is exceedingly exaggerated.

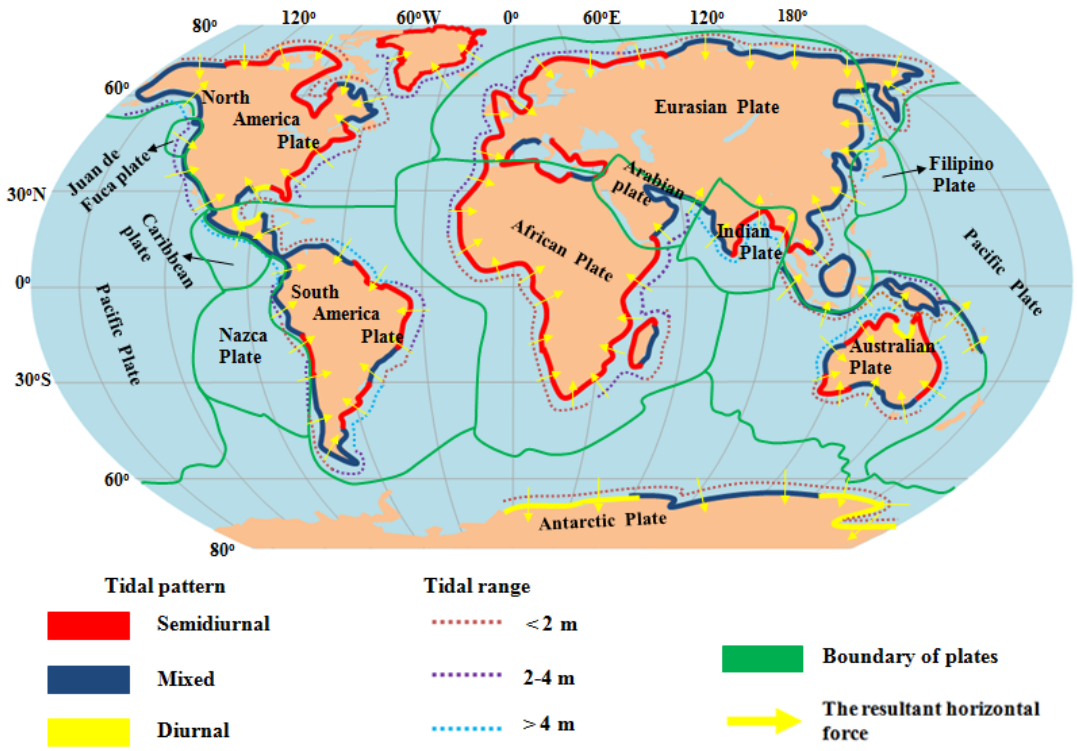

Fig. 4. A global view of the distribution of tidal pattern, tidal range, plate tectonics, and the resultant horizontally forces from ocean. Tide data supporting is from U.S. NOAA, GLOSS database - University of Hawaii Sea Level Center (Caldwell et al. 2015), and Bureau National Operations Centre (BNOC) of Australia, and tide range also refer to the times atlas of the oceans, 1983, Van Nostrand Reinhold, NY.

A quantitative treatment of the continent's movement must include more details. Practically, a continent, if not connected to another, is being surrounded by oceans, this means that the total horizontal force accepted by this continent would be a combination of the horizontal forces generated at the all sides of the continent. The spherical Earth bends the continent inevitably, this makes the horizontal forces generated unable to fall onto a plane. In addition, the tides are not synchronous in the oceans, and their amplitudes perform two cycles of large and small per month, which are related to the positions of the Sun, Moon, and Earth, and become maximal at the times of full and new Moon and minimum at the times of first quarter and last quarter. Furthermore, the loading/unloading rate of a tide is not uniform, this leads the horizontal force generated to vary at a changing rate, this varying rate also yields big difficulty in determining the time that the continent takes to accelerate and decelerate during a tide. More features of the tides may refer to these works (Pugh 1987; Pugh and Woodworth 2014). To simplify the following calculation, the continent is firstly assumed to be more rigid and planar, this allows the application of Newton mechanics to the continent's movement. We further assume all the tides circling the continent to be synchronous and their amplitudes to be constant. Based on equation (1), the total horizontal force generated would be maximal when the phase difference between the tides at both sides are 90^o whereas would be minimal when the phase difference are 0^o. The synchronous represents the phase difference $\varphi=0^o$. It may be inferred, if the total horizontal force generated under this condition (i.e., the phase difference $\varphi=0^o$) is large enough to overcome the total resistive force, naturally, the total horizontal force generated under other condition (the phase difference $\varphi\neq0^o$) has ability to overcome the total resistive force. We thus use the total horizontal force generated under the condition of the tidal phase difference $\varphi=0^o$ to acts as a lowest threshold to determine the continent's movement. We further assume the tide loading/unloading rate to be uniform, if refer to Figure 3, this indicates the time that the continents takes to accelerate is equal to the time it takes to decelerate during

a tide, namely, $t_2=t_3$. And then, according to the knowledge of Newton's 2nd law, the movement that a continent obtains within a year may be approximately written as

$$D = \mathbf{365}*\mathbf{2}*(\frac{1}{2}*\left(\frac{1}{2}*\frac{\left(F_{ocean}+F_{\mathbf{max}-tide}-F_{resistive}\right)}{M}\right)*t^{\mathbf{2}}+(\frac{1}{2}*\frac{\left(F_{ocean}+F_{\mathbf{max}-tide}-F_{resistive}\right)}{M}*t)*t$$
$$-\frac{1}{2}*\left(\frac{1}{2}*\frac{\left(F_{resistive}-F_{ocean}-F_{\mathbf{max}-tide}*\mathbf{cos}\left(\frac{3}{2}*\omega t\right)\right)}{M}\right)*t^{\mathbf{2}})$$

(2)

where F_{ocean} denotes the total horizontal force generated due to ocean and may be written as $F_{ocean}=\left((\sum_{i=1}^{n}F_{i-ocean-latitudinal})^{\mathbf{2}}+(\sum_{i=1}^{n}F_{i-ocean-longitudinal})^{\mathbf{2}}\right)^{\frac{1}{2}}$, $F_{i\text{-}ocean\text{-}latitudinal}$ and $F_{i\text{-}ocean\text{-}longitudinal}$ denote respectively the latitudinal and longitudinal forces decomposed from the horizontal force generated due to ocean at the *i*th side of a continent, and may be written as $F_{i-ocean-latitudinal}=F_{i-ocean}\sin\Omega_i$, $F_{i-ocean-longitudinal}=F_{i-ocean}\cos\Omega_i$, and $F_{i-ocean}=\mathbf{0.5\rho g}Lh_{\mathbf{ocean}}{}^{2}$, it denotes the horizontal force generated due to ocean at the *i*th side of the continent. $F_{\max\text{-}tide}$ denotes the maximal total horizontal force generated due to tide and may be written as $F_{\max-tide}=\left((\sum_{i=1}^{n}F_{i-tide-latitudinal})^{\mathbf{2}}+(\sum_{i=1}^{n}F_{i-tide-longitudinal})^{\mathbf{2}}\right)^{\frac{1}{2}}$, $F_{i\text{-}tide\text{-}latitudinal}$ and $F_{i\text{-}tide\text{-}longitudinal}$ denotes respectively the latitudinal and longitudinal forces decomposed from the horizontal force generated due to tide at the *i*th side of the continent, and may be written as $F_{i-tide-latitudinal}=F_{i-tide}\sin\Omega_i$, $F_{i-tide-longitudinal}=F_{i-tide}\cos\Omega_i$, and $F_{i-tide}=\mathbf{0.5\rho g}L\left(2h_{\mathbf{ocean}}h_{\mathbf{tide}}+h_{\mathbf{tide}}{}^{2}\right)$, it denotes the horizontal force generated due to tide at the *i*th side of a continent at the time of highest high tide. Ω_i is the inclination of the *i*th side to latitude and may be got through the geographic latitudes and longitudes of the two sites that respectively locate at the ends of this side. ρ, g, L, h_{ocean}, and h_{tide} are respectively density of water, gravitational acceleration, the continent side's width, ocean depth, and tidal height. M denotes the continent's mass and can be got through $M=S\text{d}\rho_{\text{continent}}$, where S, d, and $\rho_{\text{continent}}$ are respectively the continent's area, thickness, and density. $F_{resistive}$ denotes the total resistive force and is currently unknown, we need to value it in the calculation. ω is angular frequency and its magnitude is roughly equal to 30^{o} per hour (equal to 0.00833^{o} per second). t is the time (unit in second) that the continent takes to accelerate during a tide, and then, according to a relationship of movement, this time may be eventually expressed as

$$t=\frac{2}{3\omega}\arccos\left(\frac{2(F_{resistive}-F_{ocean})}{F_{\max-tide}}-1\right) \qquad (3)$$

The total pressure a liquid exerts includes static and dynamic pressures, the former relates to liquid's motion, while the latter is exhibited by liquid equally in all directions. In the oceans there are many kinds of currents such as Antarctic circumpolar current, deep ocean current, western boundary currents, and so on. The ebb and flow of a tide also may be treated as some

kind of current. All these currents performing liquid's motion are relatively weak in producing the dynamic pressure because of their slow speeds, we therefore neglect the force generated due to the dynamic pressure when treating the continent's movement. Practically, the side of a continent is not flat, and the continent's base is wider than its top, these make the continent look like a circular truncated cone staying in the ocean. As the horizontal force is only related to the ocean's width (i.e., the continent side's width), ocean depth, and tidal height, this suggests that we may firstly project a continent along horizontal direction into a polygonal column and divide its side into a series of smaller rectangular sides connecting one to another, and then, calculate the horizontal force generated at each of these rectangular sides, last, combine these horizontal forces to form a single horizontal force. With these theoretical ideas, we take the parameters involved to calculate the movement of a few continents (South American, African, Indian, and Australian). The controlling sites that are used to calculate the horizontal forces refers to Figure 5, the longitudes and latitudes of these sites are resolved through Google Earth software. The given values for related parameters, the horizontal forces generated, and the resultant movements are respectively listed in table 1, 2, and 3. Overall, the resultant movements for South American, African, Indian, and Australian continents are respectively 2.8, 4.2, 5.7, and 6.3 cm/yr, which are well consistent with the observed movement of generally 5.0~10.0 cm/yr (Read and Watson 1975).

Careful reader would see that in the calculation the total resistive force ($F_{resistive}$) is technically valued. This treatment, however, must be practically acceptable. As shown in Figure 1, the friction exerted by the asthenosphere along the continent's base is just one of the components of the total resistive force. In fact, the other components of the total resistive force, i.e., the push force, the pull force, and the shearing forces, are all related to the frictions generated due to the asthenosphere at the base of adjacent crusts. Thus, the friction may be a key index to examine the rationality of that treatment. The friction exerted by the asthenosphere along the continent's base may be expressed as $F_A=\mu Au/y$, where μ, A, u, and y are respectively the viscosity of the asthenosphere, the continent's area, the continent's speed, and the thickness of the asthenosphere. The viscosity and thickness of the asthenosphere vary largely according to different authors. Cathless (1971) concluded the viscosity no less than 10^{20} P, Jordan (1974) treated the thickness as 300 km. Fjeldskaar (1994) suggested that the asthenosphere has a thickness of less than 150 km and a viscosity of less than $7.0*10^{20}$ P. Some works using glacial isostatic adjustment and geoid studies concluded the asthenospheric viscosity ranges from 10^{19} to 10^{21} P (Hager and Richards, 1989; King, 1995; Mitrovica, 1996). James et al. (2009) used model to show that the asthenospheric viscosity is varied from $3*10^{19}$ P for a thin (140 km) asthenosphere to $4*10^{20}$ P for a thick (380 km) asthenosphere. We here adapt $\mu=3*10^{19}$ P and y=140 km to calculate the friction exerted by the asthenosphere for the selected four continents. The speeds of these continents (South American, African, Indian, and Australian) are valued as 2.7, 4.2, 5.6, and 6.4 cm/yr, respectively. Table 2 lists the frictions calculated for these selected continents. Evidently, for each of these continents the magnitude of the total horizontal force generated due to ocean is extremely close to that of the friction calculated. We believe this approach is not coincidence, because these two kinds of forces are got through two different passages. Such exactly approach suggests the treatment above is acceptable. The discrepancy between the total horizontal force and the friction could arise from that the related parameters cannot be exactly estimated here, for example, the solution of ocean depth through Google Earth software may yield deviation. We should remind reader that, if there were no fractures (the gaps along the ocean ridges, for instance) within ocean basin, the horizontal forces generated at all the sides of ocean basin would be balanced by the basin itself and wouldn't interact with the external force (the basal friction, for instance). It is the existence of these fractures of ocean basin to allow the horizontal force generated due to ocean to directly fight against with the friction exerted by the asthenosphere along the base of the continent.

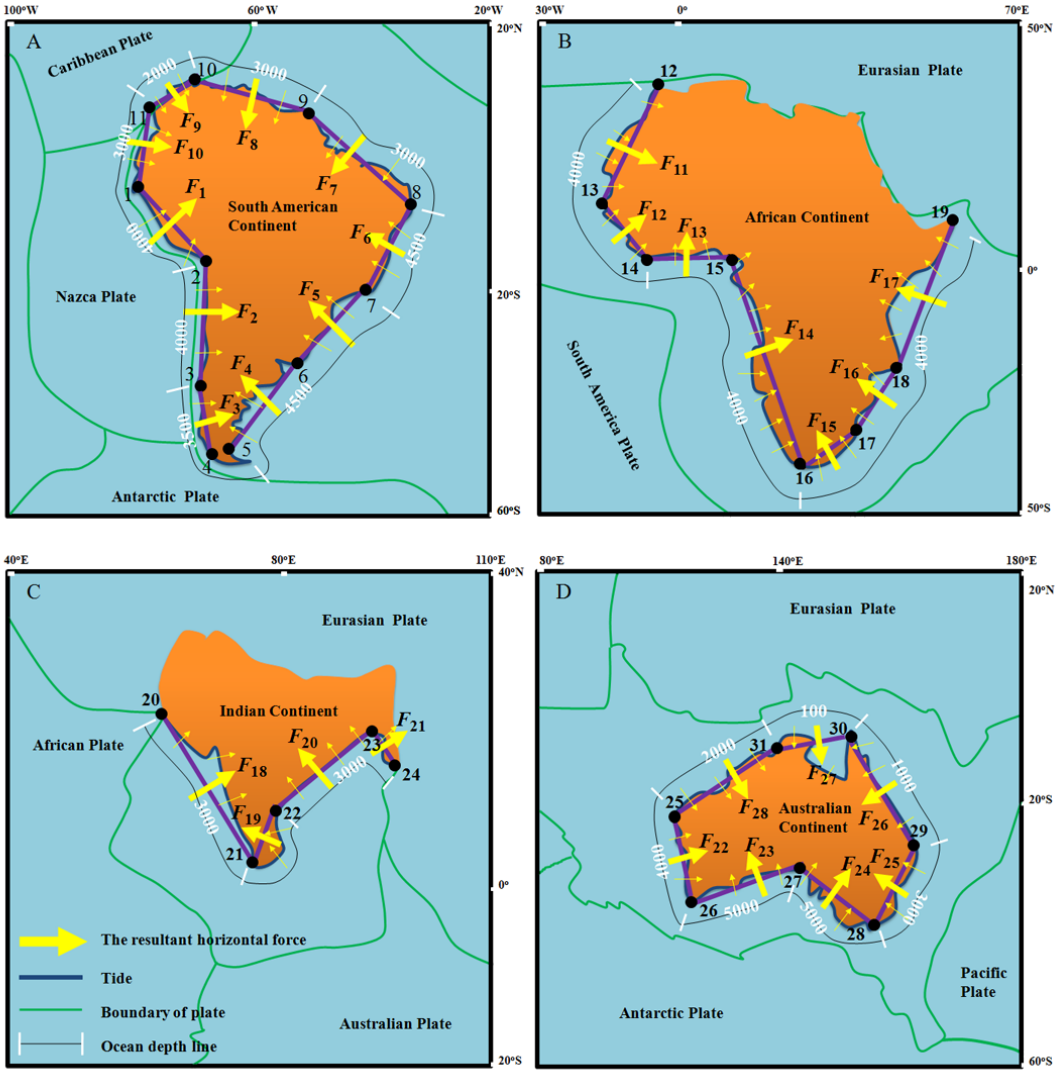

Fig. 5. Geographic treatment of the controlling sites for selected continents and the resultant horizontal forces exerted on them. *F* (yellow arrow) denotes the horizontal force generated, while purple bar denotes the distance applied by the horizontal force. The product of this distance and ocean depth is the area applied by the horizontal force. Dot with number denote controlling site. Ocean depth is artificially resolved from Google Earth software.

Table 1 Basic information for selected four continents

Continent	area	thickness	density	mass	site			site to site				tide amplitude	ocean depth
								distance		inclination to latitude, east (+)			
	S	d	ρ	M				L		i	Ω_i	h_{tide}	h_{ocean}
	km^2	km	kg/m^3	kg	No.	Longitude	Latitude	km			degree (°)	m	m
South American	17,840,000	6	3,100	3.32E+20	1	80.0°W	2.0°S	1_2	2,087	1	122.01	1.5	4,000
					2	70.0°W	18.0°S	2_3	1,153	2	73.30	1.5	4,000
					3	73.0°W	28.0°S	3_4	2,780	3	90.00	1.5	3,500
					4	73.0°W	53.0°S	5_6	2,308	4	51.15	2.0	4,500
					5	68.0°W	52.5°S	6_7	1,730	5	43.78	2.0	4,500
					6	54.0°W	34.5°S	7_8	1,952	6	64.89	1.5	4,500
					7	42.0°W	23.0°S	8_9	2,525	7	146.66	1.5	3,000
					8	34.0°W	7.0°S	9_10	2,157	8	160.64	1.5	3,000
					9	53.0°W	5.5°N	10_11	836	9	41.26	1.5	2,000
					10	72.0°W	12.0°N	11_1	1,033	10	75.66	1.5	3,000
					11	78.0°W	7.0°N						
African	30,370,000	6	3,100	5.65E+20	12	6.0°W	35.5°N						
					13	17.0°W	14.7°N	12_13	2,535	11	117.65	1.0	4,000
					14	7.0°W	4.6°N	13_14	1,531	12	45.00	1.0	4,000
					15	8.0°E	4.4°N	14_15	1,696	13	3.81	1.0	4,000
					16	22.2°E	34.7°S	15_16	4,577	14	109.75	1.0	4,000
					17	30.4°E	30.7°S	16_17	886	15	26.00	1.0	4,000
					18	40.0°E	16.0°S	17_18	1,904	16	56.85	1.0	4,000
					19	51.0°E	11.0°N	18_19	3,237	17	67.83	1.0	4,000
Indian	4,400,000	6	3,100	8.18E+19	20	66.8°E	25.0°N						
					21	77.5°E	8.0°N	20_21	2,205	18	122.19	2.0	3,000
					22	80.0°E	15.2°N	21_22	846	19	70.85	2.0	3,000
					23	91.5°E	22.7°N	22_23	1,468	20	33.11	2.0	3,000
					24	94.3°E	16.0°N	23_24	801	21	112.68	2.0	3,000

					25	114.0°E	23.0°S	25_31	2,162	28	32.43	2.0	2,000
					26	117.2°E	35.0°S	25_26	1,370	22	104.93	2.0	4,000
					27	131.0°E	31.5°S	26_27	1,340	23	14.23	1.0	5,000
Australian	8,600,000	6	3,100	1.60E+20	28	149.8°E	37.6°S	27_28	1,846	24	162.02	1.0	5,000
					29	153.0°E	25.4°S	28_29	1,390	25	75.30	2.0	3,000
					30	142.4°E	10.8°S	29_30	1,970	26	125.98	2.0	1,000
					31	131.0°E	12.2°S	30_31	1,252	27	7.00	2.0	100

Note: all geographic sites refer to Figure 5; tide amplitude is half of tidal range.

Table2 The resultant horizontal force and constrained resistive force for selected four continents

Continent	the horizontal force [a]									the total resistive force [b]	the friction [c]
	F_{ocean}					F_{tide}					
	i	horizontal	decomposed		composition	i	horizontal	decomposed		composition	$F_{resistive}$	f_{base}
			latitudinal , east (+)	longitudinal , north(+)				latitudinal , east (+)	longitudinal , north(+)			
		$F_{i\text{-}ocean}$	$F_{i\text{-}ocean\text{-}latitudinal}$	$F_{i\text{-}ocean\text{-}latitudinal}$			$F_{i\text{-}tide}$	$F_{i\text{-}tide\text{-}latitudinal}$	$F_{i\text{-}tide\text{-}latitudinal}$			
		N (*10^{17})					N (*10^{14})				N (*10^{17})	
South American	1	1.6362	1.3875	0.8672		1	1.2274	1.0408	0.6505			
	2	0.9043	0.8661	-0.2598		2	0.6783	0.6497	-0.1949			
	3	1.6686	1.6686	0.0000		3	1.4306	1.4306	0.0000			
	4	2.2905	-1.7837	1.4369		4	2.0364	-1.5859	1.2775			
	5	1.7169	-1.1879	1.2395		5	1.5264	-1.0561	1.1021			
	6	1.9365	-1.7535	0.8219		6	1.2912	-1.1692	0.5480			
	7	1.1136	-0.6121	-0.9304		7	1.1139	-0.6122	-0.9306			
	8	0.9510	-0.3153	-0.8973		8	0.9513	-0.3153	-0.8975			
	9	0.1639	0.1081	-0.1232		9	0.2460	0.1622	-0.1849			
	10	0.4555	0.4413	-0.1128		10	0.4556	0.4414	-0.1128			
			-1.1807	2.0421	2.3588			-1.0140	1.2574	1.6153	2.3604	3.2730
African	11	1.9873	1.7604	-0.9221		11	0.9938	0.8803	-0.4611			
	12	1.2000	0.8485	0.8485		12	0.6001	0.4243	0.4243			

	13	1.3298	0.0885	1.3268		13	0.6650	0.0442	0.6635			
	14	3.5882	3.3772	1.2123		14	1.7943	1.6888	0.6062			
	15	0.6949	-0.3047	0.6246		15	0.3475	-0.1524	0.3123			
	16	1.4924	-1.2496	0.8160		16	0.7463	-0.6249	0.4081			
	17	2.5379	-2.3503	0.9575		17	1.2691	-1.1753	0.4788			
			2.1700	4.8637	5.3259			1.0851	2.4322	2.6633	5.3283	8.6672
	18	0.9724	0.8230	0.5180		18	1.2970	1.0977	0.6909			
	19	0.3729	-0.3523	0.1223		19	0.4974	-0.4699	0.1631			
Indian	20	0.6474	-0.3536	0.5422		20	0.8634	-0.4717	0.7232			
	21	0.3531	0.3258	0.1362		21	0.4710	0.4346	0.1816			
			0.4429	1.3187	1.3911			0.5907	1.7589	1.8554	1.3929	1.6743
	22	1.0740	1.0377	0.2767		22	1.0743	1.0380	0.2768			
	23	1.6411	-0.4034	1.5907		23	0.6565	-0.1614	0.6363			
	24	2.2618	0.6981	2.1514		24	0.9048	0.2793	0.8607			
	25	0.6129	-0.5929	0.1555		25	0.8175	-0.7907	0.2074			
Australian	26	0.0965	-0.0781	-0.0567		26	0.3865	-0.3128	-0.2271			
	27	0.0006	0.0001	-0.0006		27	0.0248	0.0030	-0.0246			
	28	0.4237	0.2272	-0.3577		28	0.8479	0.4547	-0.7157			
			0.8887	3.7594	3.8630			0.5100	1.0138	1.1349	3.8640	3.6815

Note: all related forces refer to Figure 5.

a (the horizontal force) and *c* (the friction) are calculated, while *b* (the total resistive force) is valued.

Table 3 The resultant movements for selected four continents

Continent	movement per year	to latitudinal direction, east (+)
	mm/yr	degree
South American	27.59	120.04
African	41.85	65.96
Indian	56.46	71.44
Australian	63.09	76.70

Note: all the movement refer to Figure 5.

The treatments above are only reliable for these small-sized continents. For those larger ones like Eurasian and North American continents, their curvatures cannot be ignored, the horizontal forces generated cannot pass their barycenters, a torque effect may be generated to rotate these continents. Figure 6(A and B) conceptually demonstrates how these continents move under the torque effect of the resultantly horizontal forces.

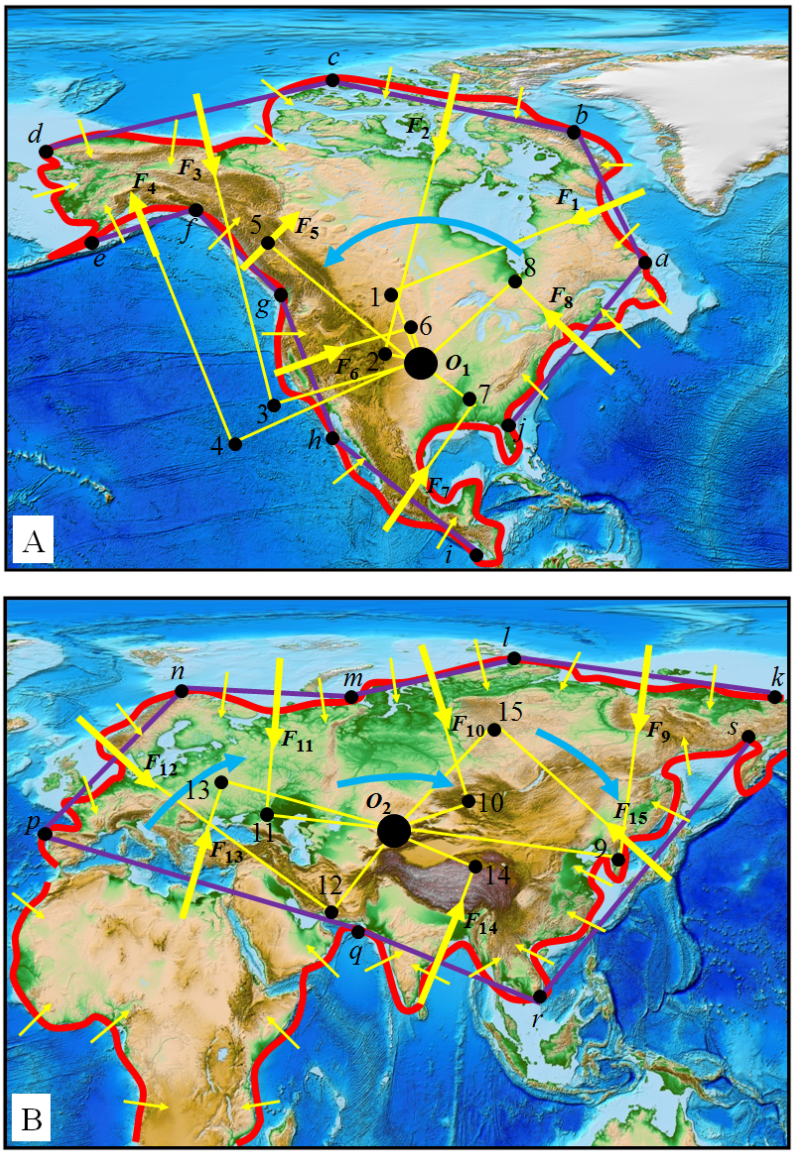

Fig. 6. Dynamics for the movements of North American and Eurasian continents. O_1 and O_2 denote possible positions for the barycenters of two continents. F_1, F_2, F_3, i.e., marking with yellow arrows, denote the horizontal forces yielded, *a*, *b*, *c*, i.e., denote the selected controlling sites, while *ab*, *bc*, *cd*, i.e., marking with purple bars, denote the length of continent's side, while $O_1$1, $O_1$2, . . ., $O_2$9, $O_2$10, i.e., denote the arms applied by the horizontal forces. Torque effect is expressed with a product of force and arm. Curved blue arrows represent some expected rotations around these barycenters. Note F_{13} actually represents a lateral push force from the tavelling African continent. The background map is produced from ETOPO1 Global Relief Model (Amante and Eakins, 2009).

2.3 Plate motion

Plate motion may be a manifestation of the horizontal force generated due to ocean. As shown in Figure 1 and Table 2, the majority of the horizontal force generated is used to fight against the resistive force that consists of the friction exerted by the asthenosphere along the continent's base, the push force from the crust at the right side, the pull force from the crust at the left side, the shearing from the crust at the far side, and the shearing from the crust at the near side. By a relationship of action and reaction, these forces (the push force, the pull force, and the shearing) further work the crusts that bear them to move, it is this process to form plate motion over the globe.

Pacific Plate's unusual motion (i.e., nearly orthogonal to Australian plate's motion) might be a consequence of the combination of two lateral pushes separately from North American Plate and from Australian Plate. As outlined in Figure 7, the northeasterly travelling Australian Plate and the rotating North American Plate respectively provide push force F_{PA} and F_{PN} to Pacific Plate, a composition of these two forces would be force F_P, which provides a dynamics for Pacific Plate. One should be aware, if plate is assumed to be more rigid, it means lateral force may transfer from one plate to another. Quantifying Pacific Plate's motion is somewhat complicated. According to the relationship of movement and force, the equation (2) may be further simplified as $F \sim DM$, where F is the total horizontal force that a continent accepts, M is the continent's mass, and D is the resultant movement. Applying this simplified relationship to South American continent, it would be $F_S \sim D_S M_S$. Furthermore, we apply this relationship to North American continent and make analogy with South American continent, there would be $F_N \sim F_S D_N M_N / D_S M_S$, where F_N and F_S denote the total horizontal force accepted respectively for North American continent and for South American continent, D_N and D_S denote the resultant movement respectively for these two continents, and M_N and M_S denote the masses of these two continents. Refer to the parameters listed in Table 1, 2, and 3, there would be F_S=2.3605*10^{17} N, D_S=2.7 cm per year, M_S=3.32*10^{20} kg. North American continent holds an area of about 24,709,000 km^2, applying the expression $M=S\mathrm{d}\rho_{\text{continent}}$ (where S, d, and $\rho_{\text{continent}}$ are respectively the continent's area, thickness, and density), the continent's mass is calculated as M_N=4.60*10^{20} kg. North American Plate (continent) rotates counter clockwise and moves with a speed of about 1.5~2.5 cm per year, we adapt D_N=2.0 cm per year for the movement at the west of this plate that interacts with Pacific Plate. And then, the total horizontal force calculated for North American continent is F_N=~2.4227*10^{17} N. To run North American Pate, the total horizontal force F_N needs to fight against the resistive force that this continent bears, which consists of mainly the push force from Pacific Plate and the shearing from South American plate. As the push force and the shearing are all related to the friction exerted by the asthenosphere along the base of these two plates, and further refer to the friction expression $F_A=\mu Au/y$ (where μ, A, u, and y are respectively the viscosity of the asthenosphere, the continent's area, the continent's speed, and the thickness of the asthenosphere), i.e., it would be $F_A \sim A$, the push force from Pacific Plate may be then linearly written as $F_{PN}= F_N S_P/(S_P+S_N)$=1.0261*10^{17} N, where S_P and S_N are respectively the area of Pacific Plate and South American Plate. Refer to table 2, the total resistive force for Australian plate is $F_{Au\text{-}resistive}$ =3.8640*10^{17} N, we assume about 25% of this force is used to fight against the push force from Pacific Plate, and then, the push force is worked out to be F_{PA}=9.6600*10^{16} N. By a the relationship of action and reaction, Pacific plate finally obtains one push force F_{PN} from North American Plate and another push force F_{PA} from Australian Plate. Australian Plate moves dominantly in a northeast direction of inclination to latitude 76.7^o, east (+), as shown in Table 3. Most of North American Plate, however, moves in roughly a southwest direction away from the Mid-Atlantic Ridge, we adapt the push force from the part of North American Plate that interacts with Pacific Plate to be in a southwest direction of inclination to latitude 190^o, east (+). The total horizontal force accepted by Pacific Plate accepts may be linearly expressed as $F_P=((F_{PN}^2+F_{PA}^2-2*F_{PN}F_{PA}*\cos(\alpha-\beta))^{0.5}$, and $\cos\gamma=(F_P^2+F_{PN}^2-F_{PA}^2)/(2*F_P*F_{PN})$, where α=76.7^o, β=10^o. Finally, it is calculated as F_P=1.096315*10^{17} N, and γ=54.03^o. Similarly, we assume that the majority of the total horizontal force accepted by Pacific Plate has been used to fight against the resistive force, which consists of mainly the friction exerted by the asthenosphere along Pacific Plate's base.

Refer to Table 2, the ratio between the total resistive force and the total horizontal force for South American continent may reach up to 0.99999907. Compared to this ratio, a ratio of 0.99999 for Pacific Plate appears to be allowable, and then, the total resistive force for Pacific Plate is calculated as $F_{Pa\text{-}resistive}$=1.096304*10^{17} N. Refer to Table 1, the continent's thickness is commonly valued as 6.0 km, the average ocean depth is less than 4.0 km, this allows a thickness of 2.0 km to be left for the continental crust to interact with the oceanic crust of same thickness. Pacific Plate's mass may be expressed as $M_{\text{Pacific}}=Sd\rho_{\text{plate}}$ (where S, d, and ρ_{plate} are respectively the plate's area, thickness, and density). If we allow the plate's density to be equal to the continent's density, and assume Pacific Plate's area to be 103,300,000.00 km^2, and then, there would be M_{Pacific}= 6.4046*10^{20} kg. The equation (2) itself may be simplified as $D \approx 365*2*(0.5*(F_{ocean}+F_{\text{max-}tide}-F_{resistive})*t^2/M)$, where $(F_{ocean}+F_{\text{max-}tide})$ denotes the total horizontal force that the continent accepts, $F_{resistive}$ denotes the total resistive force that the continent bears. According to the equation (3) and refer to Table 2, the time that Australian continent takes to accelerate within a tide is t=2*arccos(2($F_{resistive}$-F_{ocean})/$F_{\text{max-}tide}$-1)/3=378.35 s. Applying the simplified equation (2), the total horizontal force that Pacific Plate accepts, the mass of Pacific Plate, and the time that Australian continent takes to accelerate to resolve Pacific Plate's motion, it would be D=365*2*(0.5*(F_P-$F_{Pa\text{-}resistive}$)*t^2/M_{Pacific})=89.44 mm per year, a roughly northwest direction of inclination to latitude 44.03°, east (+).

Notwithstanding, if we look back North American Plate from a viewpoint of evolution, it must had rotated much during a timescale of more than millions of years, this means that North American Plate could be oriented towards northeast in the past, if so, the push force F_{PN} may be not existed at that time, Pacific Plate was most likely pushed by Australian Plate alone to move along northeast. This means that, an abrupt change in motion might had occurred for Pacific Plate at a moment when North American Plate rotated to a central angle, from which a combination of the two lateral forces considered above becomes possible. Such plate motion change has been actually witnessed by the Hawaiian–Emperor bend (Sharp and Clague, 2006; Wessel and Kroenke, 2008).

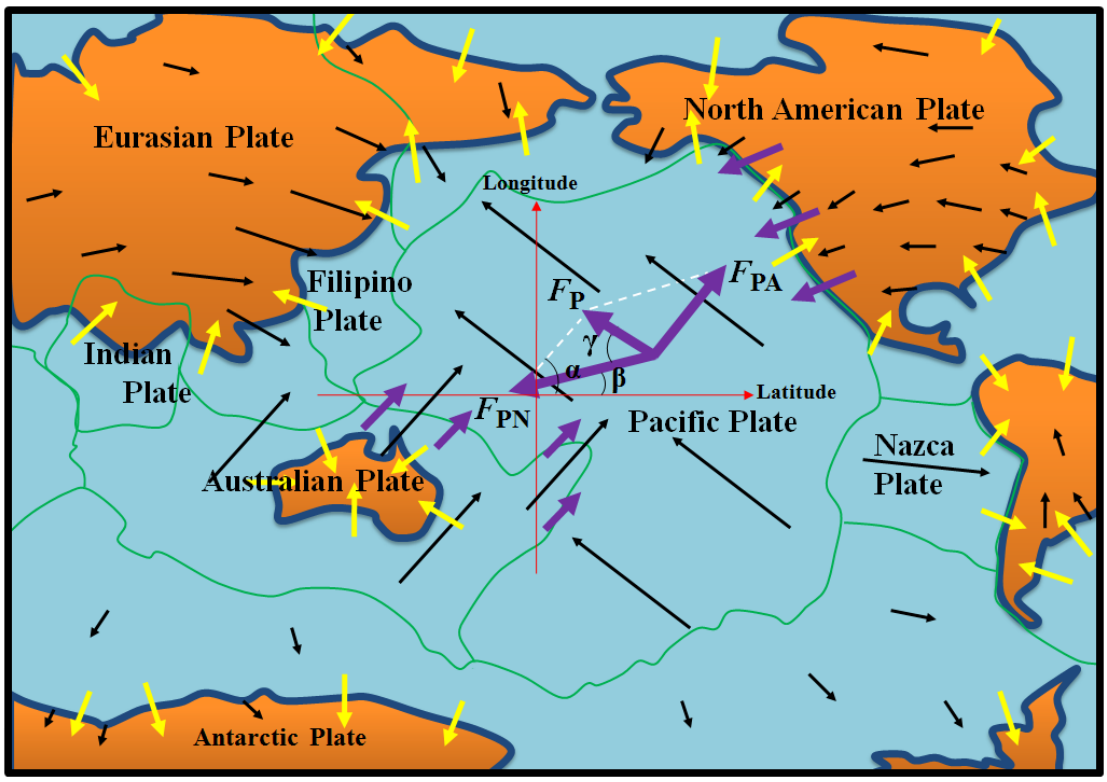

Fig. 7. Modelling the dynamics of Pacific Plate based on a combination of two lateral forces respectively from Australian and North American Plates. Black, yellow, and purple arrows denote respectively plate motions, the resultant horizontally forces, and lateral push forces from related plates. Note lateral push force F_{PN}(F_{PA}) is approximately parallel to the motion of North American (Australian) Plate.

3 Discussion

3.1 Clarification on tidal drag driving mechanism

Tidal drag proposed as a driving mechanism for plate motion had been long debated. Wegener (1924) attributed the westward drift of the American blocks to tidal drag, but Jeffreys (1929) argued that the westward stress related to tidal drag is too small to be competent for the displacement. A rapid growth of tidal drag driving mechanism arises from the confirmation of a net rotation or westward drift of the lithosphere relative to the mantle (Rittmann, 1942; Le Pichon, 1968; Bostrom, 1971; Moore, 1973), which is supported by independent observations such as plate motion within the hot spot reference frame (Ricard et al., 1991; O'Connell et al., 1991; Gordon, 1995; Gripp and Gordon, 2002), plate motion relative to Antarctica (Le Pichon, 1968; Knopoff and Leeds, 1972), and supported by geological asymmetries (Doglioni, 1993). Another supporting to it comes from energy budget. For instance, many works calculated that tidal drag is energetically feasible for plate motion. According to Rochester (1973) and Jordan (1974), the total energy released due to tidal friction exceeds $5*10^{19}$ ergs/s, excluding the dissipation in both shallow seas and solid Earth (Miller, 1966; Munk, 1968), a remaining energy of about $3*10^{19}$ ergs/s might be available for driving plate motion, this amount exceeds by 2 orders of magnitude the lower bound set by seismic energy release (Gutenberg, 1956). Some authors (Egbert and Ray, 2000; Ray, 2001; Riguzzi et al., 2010) recently reevaluated the energy budget to show that the total energy released by tidal friction may reach up to $1.2*10^{20}$J/yr, subtracting the dissipation in the mantle, oceans, and shallow seas, a residual energy of about $0.4*10^{20}$J/yr is larger than the one required to maintain the net rotation, estimated at about $1.27*10^{19}$J/yr. Nevertheless, a satisfaction in energy supply cannot shield tidal drag driving mechanism. Both Jordan (1974) and Jeffreys (1975) seriously attacked the theoretical basis of tidal drag driving mechanism, they claimed that the viscosity both related to tidal drag and necessary to allow decoupling between lithosphere and mantle ($\sim 10^{11}$ Pas) is far less than the present-day asthenosphere viscosity, estimated at between 10^{17} and 10^{20} Pas (Anderson, 1989; Pollitz et al., 1998; Fjeldskaar, 1994; Giunchi et al., 1997; Piersanti, 1999). Ranalli (2000) further showed that any non-zero torque due to difference in angular velocity between the mantle shell and lithosphere shell would be extremely transient, and cannot be a factor in the origin of the westward drift of the lithosphere. In spite of these arguments, tidal drag driving mechanism doesn't stop growing up. Scoppola et al. (2006) proposed the westward rotation of the lithosphere as the consequence of a combined effect of tidal torque acting on the lithosphere, downwelling of the denser material toward the deeper interior of the Earth, and thin layers of very low viscosity hydrate channels occurring in the asthenosphere. Some recent works show that, by assuming an ultra-low viscosity layer in the upper asthenosphere, the horizontal component of the tidal oscillation and torque have ability to move the lithosphere (Riguzzi et al., 2010; Doglioni and Panza, 2015).

Comparing the tidal drag driving mechanism and the ocean-generating force driving mechanism presented in this work, we may pick up a few points to share that, first of all, the tidal drag driving mechanism is to explain the westward drift of the lithosphere relative to the mantle, while the latter is proposed to primarily explain the present-day plate motions and related terrestrial activities (lately, we shall further show how these activities form under the effect of the ocean-generating force); Secondly, the tidal drag driving mechanism has no objection to the established plate driving forces such as slab-pull, ridge push, basal drag, and slab suction, and therefore, tidal drag may thus be thought to be some supplementary to these established forces. Contrary to this, the ocean-generating force driving mechanism treats the ocean-generating force as the dominant plate driving force. Lastly, in the paradigm of the ocean-generating force driving mechanism the horizontal force generated due to tide is rather

small relative to the horizontal force generated due to ocean, but its effect mayn't be underestimated. The total horizontal force generated due to tide for South American continent is $1.6153*10^{14}$ N, less than by 3 orders of magnitude of the horizontal force generated due to ocean. The significance of tide lies at it helps ocean to yield a varying horizontal force, a combination of this varying horizontal force and the resistive force (consisting mainly of basal friction) forms a discontinuous force, by which the continent obtains a steadily movement. To some extent, tide exerts some kind of launching and braking mechanism for the continent's movement. Even so, it is presently uncertain whether the ocean-generating force may be responsible for the westward drift of the lithosphere or not, this must be left to determine until a globally ocean-generating force is evaluated.

3.2 Restation on the ocean-generating force

Some authors could argue that, by means of a comparison of the magnitude between the ocean-generating force and the ridge push (also slab pull), the ocean-generating force appears to be insignificant. Such a comparison is inadequate. On the one hand, one mayn't use magnitude as a rule or criteria to determine whether a force is significant or not. As we demonstrated in the section 2, the Newton's 2nd law ($F=Ma$, $D=0.5at^2$, where F, M, a, and t are respectively the force that an object accepts, the object's mass, the resultant acceleration, and the time that the object takes to move) shows that an object's movement is related to both the magnitude of force and the time that the force exerts on the object. In other words, if one gives the object a smaller force but a relatively longer time, the object still may run a long distance. On the other hand, the applicability of force should be considered as the first factor to judge the significance. As we demonstrated in the section 1, both the ridge push and slab pull are workable only for a few plates (Nazca and Caribbean, for instance) that are either without a continent's loading or being sunken at the trench. For most of plates (African, Eurasian, North American, and South American, for instance), the available force for them is the basal drag. But unfortunately, the effectiveness of this force is presently still in a state of debate. In contrast, the ocean-generating force, which is globally distributed, may be available for all the plates.

3.3 Extension of the continent's movement

The travelling continent (i.e., the continental crust) drags its adjoining oceanic crust, this inevitably generates strain for the latter. A periodically fracture of the oceanic crust might have created the Mid-Oceanic Ridge (MOR). As shown in Figure 8, the accumulated strain eventually rips the oceanic crust as the continent continues to move, this allows the magma from the deep to erupt. The erupted magma further cools by ocean to crystallize and form new crusts. The newly formed crusts in turn may seal the fracture to terminate that eruption. The fracture temporarily relieves strain, but as the horizontal force generated continues to push the continent to move, strain is again accumulated, the following fracture and closeness occur again. The newly formed crusts add height to the oceanic crust, forming the MOR. In addition, as shown in Figure 1, the travelling continent provides not only pull to the crust at the left side, but also push to the crust at the right side and shearing to the crusts at the far and near sides of the continent, these pushes or shearing or both from different directions to identical crust also may cause the crust to fracture, allowing magma to erupt to form the MOR.

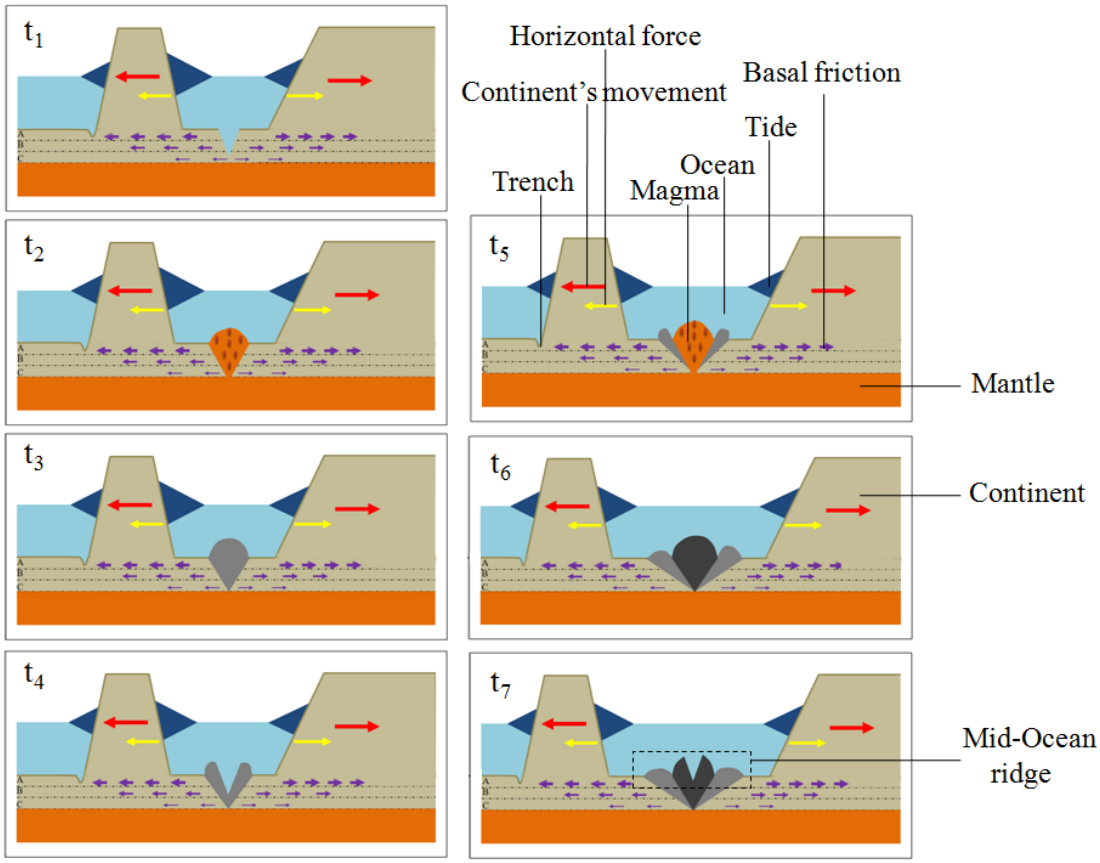

Fig. 8. Modelling the formation of MOR under the ocean-generating forces. From t_1, t_2, …, to t_7, it exhibits a sequence of the oceanic crust's evolution. The lower part of the lithosphere is apparently divided into three layers A, B, and C, so as to depict different motions due to the drag exerted by basal friction.

The overriding of a continental crust onto an oceanic crust may create a squeeze effect to the latter, creating terrestrial features/activities like trench, Earthquake, and volcano at the zones where they meet each other. Continents sits within ocean, the horizontal forces generated due to ocean push all the sides of the continent inwards, these compressions inevitably force the continent to form some folded mountains and rifts. For example, refer to Figure 9, the horizontal force pushes Indian continent impinging into Eurasian continent, as the force is almost vertical to the continental slope, this provides a bulldozer effect to uplift the materials in the front, forming the Himalayas. It should be noted that, the Himalayas was long thought to be a result of the collision of Indian Plate and Eurasian Plate. This understanding, however, is not exactly correct. These two plates have same rock density, the collision between them would result in an addition of height. The thickness of the continental (oceanic) crust is about 35 (6) km (Turcotte & Schubert 2002), an overlay of these two plates would be expected to yield a thickness of at least 80 km, regardless of the folded situation generated by plate itself and the early formed oceanic crust in the middle of the two ancient separated plates. Unfortunately, the present-day Himalayas (Mount Everest, 8,848 m) is still too low to reach this requisite height. In contrast, if we consider the Himalayas as a consequnce of the collision of the two continents, it appears to be practicable. Both the Arabian Sea and Bay of Bengal hold a depth of about 4,000 m, it is a continent's side of such depth to accept the horizontal force generated. Indian continent holds a height of no more 500 m, while Tibetan Plateau holds a height of about 4,000~5,000 m, if we add a continent of 4,000 m depth, which is equal to the sea depth that generates the horizontal force, onto Tibetan Plateau, the requisite height may be roughly got. Actually, the Himalayas provides a good reference to understand the

formation of the Alps. The Alps could arise from a collision of the travelling Italian island and other part of Europe. A major reason is the relatively deeper Ionian and Tyrrhenian seas provide more horizontal force to the side of Italian island, this gives the island a dominantly lateral push along northwest direction.

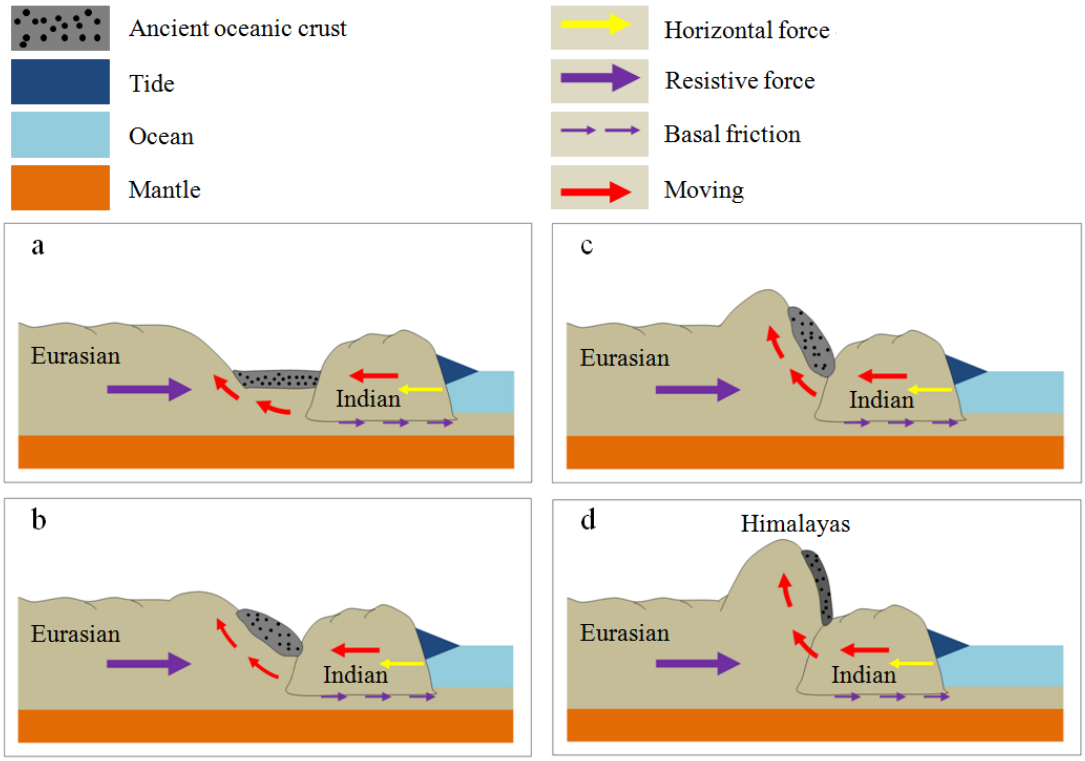

Fig. 9. Modelling the formation of the Himalayas under the collision of Indian continent and Eurasian continent. From a, b, …, to d, it shows a time sequence of the formation.

One of the most unusual features around the MOR is the transform faults which cut the ridge into a train of smaller sections, but the formation of this structure remains in a state of debate among scientific community (Gerya, 2012). The currently accepted view believes that the oceanic transform faults originated from plate fragmentation that is related to pre-existing structures (Wilson, 1965; Oldenburg and Brune, 1972; Cochran and Martinez, 1988; McClay and Khalil, 1998; Choi et at., 2008). Gerya (2010) recently theorized the transform fault of Mid-Atlantic Ridge, and concluded (Gerya, 2012) that the asymmetric crustal growth at mid-oceanic ridge can create some transform faults, while others can form earlier during the onset of oceanic spreading. A distinguishable feature of the transform fault is there are many long and nearly-parallel structures that generally across the ridge to exert the cutting, this suggests that the ridge's formation is most possibly later than the formation of these structures. We here consider a solution for the transform faults at the Mid-Atlantic Ridge. As exhibited in Figure 10, the early Atlantic is relatively narrow, the horizontal forces generated continue to push the landmasses, forcing these landmasses to gradually depart from each other, the travelling landmasses further drag the continental crust beneath them and the adjoining oceanic crust, the accumulated strain finally splits the oceanic crust into smaller nearly-parallel segments. The narrowness of the oceanic crust initially facilitates some nearly latitudinal fractures to occur. With the passage of time, the oceanic crust is increasingly expanded due to the opposed movements of the landmasses at the two sides, this fosters some longitudinal fractures to occur. For each of these segments, the leading drag to it is generally exerted along nearly opposed directions, the accumulated strain has to fracture it in the middle.

Finally, a ridge is formed for a segment, a connection of the ridges of all these segments forms the transform faults of the Mid-Atlantic Ridge.

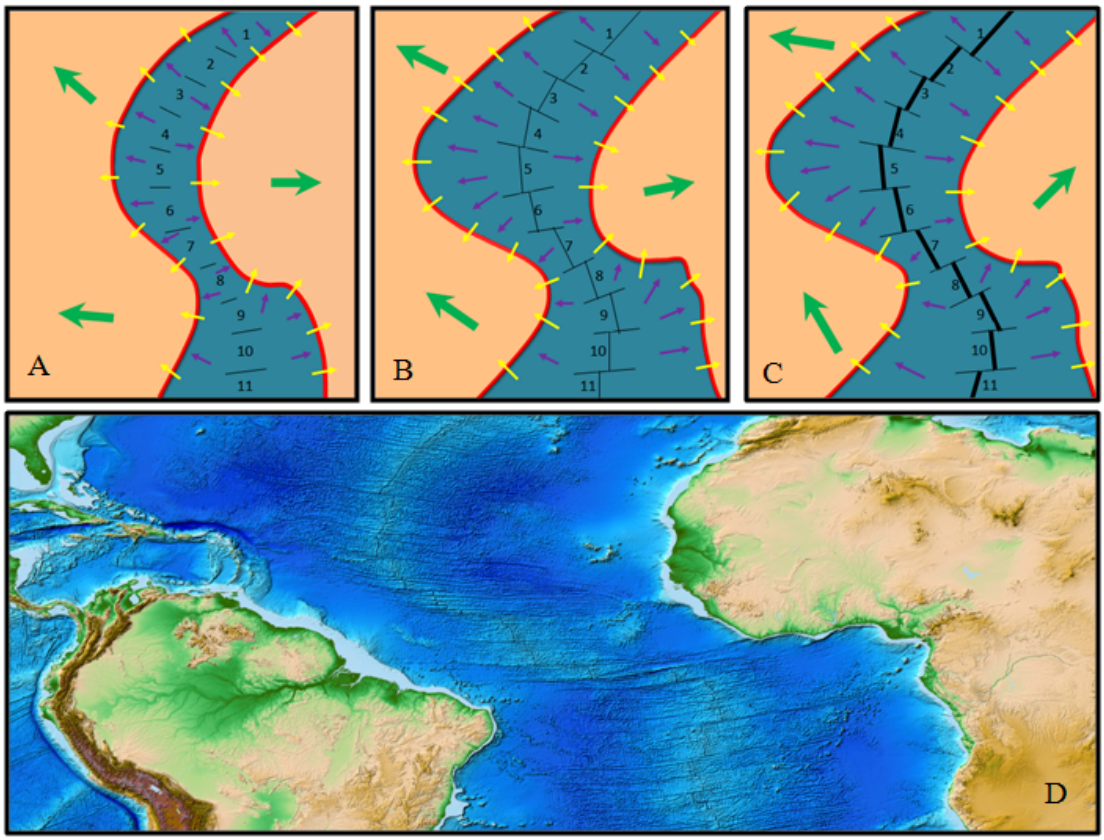

Fig. 10. Modelling the formation of MOR and transform faults. A, B, and C exhibit a sequence of how transform faults evolve with the growth of the MOR. Yellow, green, and purple arrows denote respectively the horizontal forces, the resultant movements, and the drags exerted by the travelling continents to the oceanic crust. The thin black lines represent nearly-parallel structures. Number 1, 2, . . ., and 11 represent the fragments of the oceanic crust, which consist of the section of transform faults. D shows the transform faults over the Mid-Atlantic Ridge. The background map is produced from ETOPO1 Global Relief Model (Amante and Eakins, 2009).

3.4 Reexposure of the mantle dynamics

The biggest bottleneck of the mantle dynamics lies at that it seriously fights against the established understanding of the dispersal of supercontinent, which had been thought to form presently smaller continents. Since the basal drag exerted by the mantle convection currents is always at the base of the lithosphere, if it were this basal force to split the lithosphere, the lithosphere should had been split from bottom to top. The volcano's eruption agrees that a deeper lithosphere's fracture would lead magma to rise up to the Earth's surface, after cooling, the magma's remnants would in turn occupy the room of that fracture. Similarly, if American continent and African continens were separated due to the basal drag splitting the lithosphere, the fracture must be deeper, the resultant magma's remnants would then occupy the room of the fracture, this disallows a large body of water to enter and form the Atlantic ocean. Moreover, the MOR reflects a fact that, once the lithosphere's fracture is deeper enough to contact mantle, ocean water cannot block magma from erupting. These trend to support that the dispersal of supercontinent mayn't be a consequence of the deeper fracture of the lithosphere. In fact, both African Great Rift Valley and Iceland's Rift Valley are strong evidence to support that the lithosphere's fracture is rather shallow. Different from the way that the mantle dynamics works on the lithosphere, the ocean-generating force works always at the top of the lithosphere, the result is necessarily a shallower fracture of the lithosphere.

Such a shallower fracture not only avoids the magma's eruption but also keeps room for water to enter and form ocean. The ocean-generating force driving mechanism provides line for us to conceptually track the dispersal of supercontinent. Refer to Figure 11, at the time of upper carboniferous the opening at the east of the landmass at first facilitates a large body of water to occur, the horizontal force generated pushes the adjoining landmass to move away from each other. This in turn expands the opening further. With the passage of time, the landmass was gradually broken and displayed the shape at the time of Eocene. This, again, facilitates more water to enter, and also more the horizontal force to be generated. We speculate, it is such a positive feedback to control the landmass's initial dispersal. The landmass was almost broken up at the time of the older quaternary, a relatively primitive layout of the separated continents was formally established. After that, the horizontal force continued to push the continents to move away from each other until present. Some could argue that the horizontal force circling the supercontinent would trend to compress the supercontinent other than to separate it. Our understanding lies at that, every opening at the landmass may create some kind of mechanism for a deeper fracture to occur, this allows to form a deeper water, by which a larger horizontal force is generated to effectively fight against the horizontal force that surrounds the landmass, the landmass may therefore be separated.

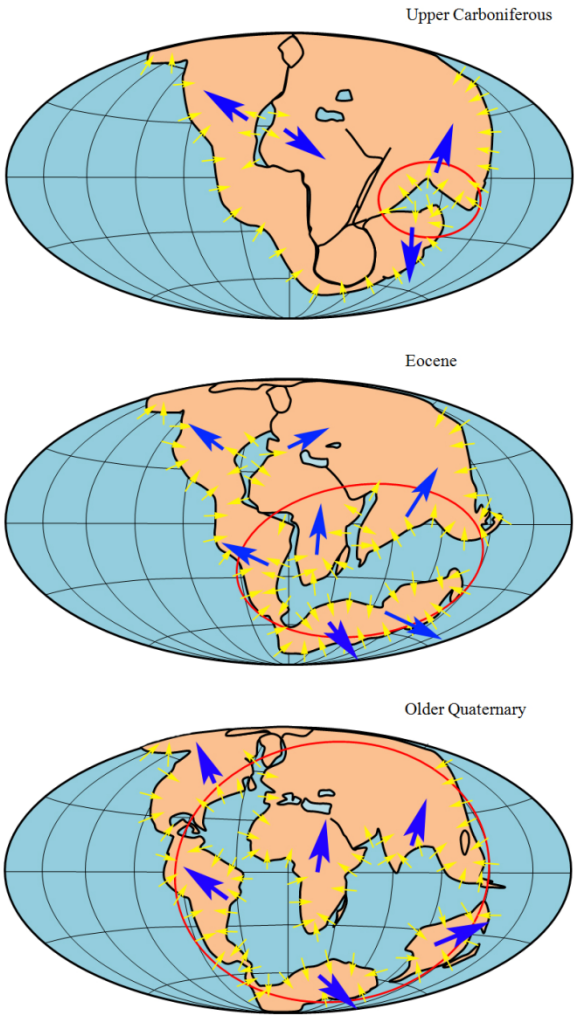

Fig. 11. Modeling the dispersal of supercontinent. Yellow and blue arrows denote respectively the horizontal forces and the resultant movements. Red circles represent an expansion of the ocean among the landmasses. The background map is yielded referring to Wegener's work (1924).

Another bottleneck of the mantle dynamics is that it evidently conflicts with the knowledge of fluid mechanics. In general, in a system a wheel-like heat convection depends a condition that the system's bottom is heated locally but not wholly. Otherwise, all the fluids heated would commonly rise up to the top of the system, this doesn't allow to form a density gradient along horizontal direction. Without such a density gradient, it wouldn't form a horizontal movement. Simply, a local heating exerted at the system's bottom is needed for yielding the wheel-like convection. The mantle dynamics ascribes the energy source of plate motion to radiogenic heating and the Earth's core cooling (Bercovic, et al., 2015). Radiogenic heating arises from a release of heat energy from the radioactive decay of radiogenic nuclides. Nevertheless, there is much uncertainty for the distribution of radiogenic nuclides in the mantle. Even if we assume the distribution of nuclides to be uneven at the time when the Earth was created, an unremitting mantle convection still trends to mix the nuclides into uniform during a timescale of billions of years. The Earth's core cooling would provide a spherically distributed heat, and thus, the mantle would be heated by this heat along its base. These disadvantages determine the wheel-like mantle convection to be impracticable.

Many people feel extraordinarily perplexed why the Earth has plate tectonics but her twin Venus does not. A large number of works had addressed that water provides right conditions (maintaining a cool surface, for instance) for the Earth's plate tectonics, while the loss of water on the Venus prohibits plate formation (Hilairet et al., 2007; Korenaga, 2007; Lenardic and Kaula, 1994; Tozer, 1985; Hirth and Kohlstedt, 1996; Lenardic et al., 2008; Landuyt and Bercovici, 2009; Driscoll and Bercovici, 2013). This work expands such understanding further, no water on the Venus, no the ocean-generating force, of course, no formation of plate tectonics on that planet.

To the end, it may be safe to say, the ocean-generating force driving mechanism presented may help extend our understanding of Earth's dynamics. Furthermore, under the effect of the ocean-generating force, a dynamic tracking of the continent's movement and an exactly prediction of Earthquake become possible. Also, the continent's movement driven by the ocean-generating force also may couple with the climate cycles supported by record from ice core and marine sediment (Petit, J. R. et al., 1999; Imbrie, J. et al., 1993; Bassinot, F. C. et al., 1994).

Acknowledgments We express honest thanks to Jeroen van Hunen, Thorsten Becker, and Carlo Doglioni for their suggestive comments. The data used are listed in the references, tables, and supplements.

References

Amante, C. and Eakins, B.W. (2009). ETOPO1 1 Arc-Minute Global Relief Model: Procedures, Data Sources and Analysis. NOAA Technical Memorandum NESDIS NGDC-24. National Geophysical Data Center, NOAA. doi:10.7289/V5C8276M.

Anderson, D.L. (1989). Theory of the Earth. InBlackwell, pp. 1-366.

Backus, G., Park, J. & Garbasz, D. (1981). On the relative importance of the driving forces of plate motion. Geophys. J. R. astr. Soc., 67,415-435.

Bassinot, F. C. et al. (1994). The astronomical theory of climate and the age of the Brunhes–Matuyama magnetic reversal. Earth Planet. Sci. Lett., 126, 91-108.

Bercovici, D. (1993). A simple model of plate generation from mantle flow. Geophysical Journal International, 114, 635-650.

Bercovici, D. (1995b). A source-sink model of the generation of plate tectonics from non-Newtonian mantle flow. Journal of Geophysical Research, 100, 2013-2030.

Bercovici, D., Tackeley, P. J., and Ricard, Y. (2015). The generation of plate tectonics from mantle dynamics. Reference Module in Earth Systems and Environmental Science: Treatise on Geophysics (Second Edition), 7, 271-318.

Bokelmann, G. H. R. (2002). Which forces drive North America? Geology, 30(11), 1027-1030.
Bostrom, R. C. (1971). Westward displacement of the lithosphere. Nature, 234, 536-538.
Cadek, O., Ricard, Y., Martinec, Z., and Matyska, C. (1993). Comparison between Newtonian and non-Newtonian flow driven by internal loads. Geophysical Journal International, 112, 103-114.
Caldwell, P. C., Merrfield, M. A., Thompson, P. R. (2015). Sea level measured by tide gauges from global oceans — the Joint Archive for Sea Level holdings (NCEI Accession 0019568), Version 5.5, NOAA National Centers for Environmental Information, Dataset, doi:10.7289/V5V40S7W.
Cathies, L. (1971). The viscosity of the Earth's mantle, Ph.D. thesis, Princeton Univ., Princeton, N.J.
Choi, E., Lavier, L., Gurnis, M. (2008). Thermomechanics of mid-ocean ridge segmentation. Phys. Earth Planet. Inter., 171, 374-386.
Christensen, U., Harder, H. (1991). Three-dimensional convection with variable viscosity. Geophysical Journal International, 104, 213-226.
Cochran, J. R., Martinez, F. (1988). Evidence from the northern Red Sea on the transition from continental to oceanic rifting. Tectonophysics, 153, 25-53.
Conrad, C. P., Lithgow-Bertelloni, C. (2002). How Mantle Slabs Drive Plate Tectonics. Science, 298 (5591), 207–09.
Doglioni, C. (1993). Geological evidence for a global tectonic polarity. Journal of the Geological Society of London, 150, 991-1002.
Doglioni, C., and Panza, G. (2015). Polarized Plate Tectonics. Advances in Geophysics, 56, 1-168.
Driscoll, P. and Bercovic, D. (2013). Divergent evolution of Earth and Venus: Influence of degassing, tectonics, and magnetic fields. Icarus. 226, 1447-1464.
Egbert, G.D., Ray, R.D. (2000). Significant dissipation of tidal energy in the deep ocean inferred from satellite altimeter data. Nature, 405, 775-778.
Fjeldskaar, W. (1994). Viscosity and thickness of the asthenosphere detected from the Fennoscandian uplift. Earth and Planetary Science Letters, 126, 399-410.
Forsyth, D. & Uyeda, S. (1975). On the relative importance of the driving forces of plate motion. Geophysical Journal International, 43, 163-200.
Gerya, T. (2010). Dynamical Instability Produces Transform Faults at Mid-Ocean Ridges. Science, 329, 1047–1050.
Gerya, T. (2012). Origin and models of oceanic transform faults. Tectonophysics, 522-523, 34-54.
Giunchi, C., Spada, G., and Sabadini, R. (1997). Lateral viscosity variations and post-glacial rebound: Effects on present-day VLBI baseline deformations. Geophysical Research Letters, 24, 13-16.
Gordon, R.G. (1995). Present plate motions and plate boundaries, in Arhens, T.J., ed., Global Earth physics, Reference Shelf 1: Washington, D.C., American Geophysical Union, p. 66-87.
Gripp, A.E., and Gordon, R.G. (2002). Young tracks of hot spots and current plate velocities. Geophysical Journal International, 150, 321-361.
Gutenberg, B. (1956). The energy of Earthquakes. Quart. J. Geol. Soc. London, 112, 1-14.
Hager, B. H., and Richards, M. A. (1989). Long-wavelength variations in Earth's geoid: Physical models and dynamical implications. Philosophical Transactions of the Royal Society of London, Series A, 328, 309-327.
Hales, A. (1936). Convection currents in the Earth. Monthly Notice of the Royal Astronomical Society, Geophysical Supplement, 3, 372-379.
Hess, H. H. (1962). History Of Ocean Basins, in Engel, A. E. J., James, H. L., & Leonard, B. F., eds. Petrologic Studies: A volume in honor of A. F. Buddington. Boulder, CO, Geological Society of America, 599-620.
Hilairet, N., Reynard, B., Wang, Y., et al. (2007). High-pressure creep of serpentine, interseismic deformation, and initiation of subduction. Science, 318(5858), 1910-1913.

Hirth, G. and Kohlstedt, D. (1996). Water in the oceanic upper mantle: Implications for rheology, melt extraction and the evolution of the lithosphere. Earth and Planetary Science Letters, 144, 93-108.
Holmes, A. (1931). Radioactivity and Earth Movements. Nature, 128, 496-496.
Imbrie, J. et al. (1993). On the structure and origin of major glaciation cycles. 2. The 100,000-year cycle. Paleoceanography, 8, 699-735.
James, T. S., Gowan, E. J., Wada, L., and Wang, K. L. (2009). Viscosity of the asthenosphere from glacial isostatic adjustment and subduction dynamics at the northern Cascadia subduction zone, British Columbia, Canada. Journal of Geophysical Research: Solid Earth,114(B4), CiteID B04405.
Jeffreys, H. (1929). The Earth,2 nde d., p. 304, Cambridge University Press, London.
Jeffreys, H. (1975). The Earth. Cambridge, Cambridge University Press, pp. 1-420.
Jordan, T. H. (1974). Some comments on tidal drag as a mechanism for driving plate motions. J. Geophys. Res., 79, 2141-2142.
King, S. D. (1995). The viscosity structure of the mantle. In Reviews of Geophysics (Supplement) U.S. Quadrennial Report to the IUGG 1991-1994, 11-17.
Knopoff, L., and Leeds, A. (1972). Lithospheric momenta and the deceleration of the Earth. Nature, 237, 93-95.
Korenaga, J. (2007). Thermal cracking and the deep hydration of oceanic lithosphere: A key to the generation of plate tectonics? Journal of Geophysical Research 112(B5), DOI: 10.1029/2006JB004502.
Landuyt, W. and Bercovici, D. (2009). Variations in planetary convection via the effect of climate on damage. Earth and Planetary Science Letter, 277, 29-37.
Lenardic, A., Jellinek, M., and Moresi, L-N. (2008). A climate change induced transition in the tectonic style of a terrestrial planet. Earth and Planetary Science Letters, 271, 34-42.
Lenardic, A. and Kaula, W. (1994). Self-lubricated mantle convection: Two-dimensional models. Geophysical Research Letters, 21, 1707-1710.
Le Pichon, X. (1968). Sea-floor spreading and continental drift. Journal of Geophysical Research, 73, 3661-3697.
McClay, K., Khalil, S. (1998). Extensional hard linkages, eastern Gulf of Suez, Egypt. Geology, 26, 563-566.
Miller, G. R. (1966). The flux of tidal energy out of the deep oceans. J. Geophys. Res., 71, 2485-2489.
Mitrovica, J. X. (1996). Haskell (1935) revisited. Journal of Geophysical Research, 101, 555–569.
Moore, G. W. (1973). Westward tidal lag as the driving force of plate tectonics. Geology, 1, 99-101.
Munk, W. H. (1968). Oncea gain-tidal friction,Q uart.J . Roy.A stronS. oc., 9, 352-375.
O'Connell, R., Gable, C.G., and Hager, B. (1991). Toroidal-poloidal partitioning of lithospheric plate motions, in Sabadini, R., et al., eds., Glacial isostasy, sea-level and mantle rheology: Dordrecht, The Netherlands, Kluwer Academic Publisher, 334, 535-551.
Oldenburg, D. W., Brune, J. N. (1972). Ridge transform fault spreading pattern in freezing wax. Science, 178, 301-304.
Oxburgh, E. and Turcotte, D. (1978). Mechanisms of continental drift. Reports on Progress in Physics, 41, 1249-1312.
Perkeris, C. (1935). Thermal convection in the interior of the Earth. Monthly Notices of the Royal Astronomical Society, Geophysical Supplement, 3, 343-367.
Petit, J. R. et al. (1999). Climate and atmospheric history of the past 420,000 years from the Vostok ice core, Antarctica. Nature, 399, 429–436.
Piersanti, A. (1999). Postseismic deformation in Chile: Constraints on the asthenospheric viscosity. Geophysical Research Letters, 26, 3157-3160.
Pollitz, F.F., Buergmann, R., Romanowicz, B. (1998). Viscosity of oceanic asthenosphere inferred from remote triggering of Earthquakes. Science, 280, 1245-1249.
Pugh, D. T. (1987). Tides, Surges and Mean Sea-Level. JOHN WILEY & SONS.

Pugh, D. T. and Woodworth, P. L. (2014). Sea-Level Science: Understanding Tides, Surges Tsunamis and Mean Sea-Level Changes. Cambridge Univ. Press, Cambridge.
Ranalli, G. (2000). Westward drift of the lithosphere: not a result of rotational drag. Geophys. J. Int. 141, 535-537.
Ray, R. (2001). Tidal friction in the Earth and Ocean. Journées Luxembourgeoises de Géodynamique´JLG 89th, Nov. 12-14, http://www.ecgs.lu/.
Read, H. H. & Watson, J.(1975). Introduction to Geology. New York, Halsted, pp13-15.
Ricard, Y., Doglioni, C., and Sabadini, R. (1991). Differential rotation between lithosphere and mantle: A consequence of lateral viscosity variations. Journal of Geophysical Research, 96, 8407-8415.
Riguzzi et al. (2010). Can Earth's rotation and tidal despinning drive plate tectonics? Tectonophysics, 484, 60-73.
Rittmann, A. (1942). Zur thermodynamik der orogenese. Geologische Rundschau, 33, 485-498.
Rochester, M.G. (1973). The Earth's rotation, EOS, T rans. Am. geophys. Un., 54, 769-780.
Runcorn, S. (1962a).Towards a theory of continental drift. Nature,193, 311-314.
Runcorn, S. (1962b). Convection currents in the Earth's mantle. Nature, 195, 1248-1249.
Scoppola, B., Boccaletti, D., Bevis, M., Carminati, E., Doglioni, C. (2006). The westward drift of the lithosphere: a rotational drag? Bull. Geol. Soc. Am. 118 (1/2), 199-209.
Sharp, W. D. and Clague, D.A. (2006). 50-Ma Initiation of Hawaiian–Emperor bend records major change in Pacific plate motion. Science, 313(5791): 1281-1284.
Spence, W. (1987). Slab pull and the seismotectonics of subducting lithosphere. Reviews of Geophysics, 25 (1), 55–69.
Stein, C., Schmalzl, J., Hansen, U. (2004). The effect of rheological parameters on plate behavior in a self-consistent model of mantle convection. Physics of the Earth and Planetary Interiors, 142, 225-255.
Tackley, P. (1998). Self-consistent generation of tectonic plates in three-dimensional mantle convection. Earth and Planetary Science Letters, 157, 9-22.
Tanimoto, T., Lay, T. (2000). Mantle dynamics and seismic tomography. Proceedings of the National Academy of Sciences, 97 (23),12409–12410.
Tozer, D. (1985). Heat transfer and planetary evolution. Geophysical Surveys, 7, 213-246.
Trompert, R., Hansen, U. (1998). Mantle convection simulations with reheologies that generate plate-like behavior. Nature, 395, 686-689.
Turcotte, D.L., and Oxburgh, E. (1972). Mantle convection and the new global tectonics. Annual Review of Fluid Mechanics, 4, 33-66.
Turcotte, D. L., Schubert, G. (2002). Plate Tectonics. Geodynamics (2 ed.). Cambridge University Press. pp.1-21. ISBN 0-521-66186-2.
Vine, F. J., & Matthews, D. H. (1963). Magnetic Anomalies Over Oceanic Ridges. Nature, 199, 947-949.
Wegener, A. (1915). The Origin of Continents and Oceans. New York, NY: Courier Dover Publications.
Wegener, A. (1924). The origin of continents and oceans (Entstehung der Kontinente und Ozeane). Methuen & Co.
Weinstein, S. (1998). The effect of convection planform on the toroidal-poloidal energy ratio. Earth and Planetary Science Letters, 155, 87-95.
Wessel, P. & Kroenke, L.W. (2008). Pacific absolute plate motion since 145 Ma: An assessment of the fixed hot spot hypothesis. Journal of Geophysical Research - Solid Earth 113(B6). http://dx.doi.org/10.1029/2007JB005499.
White, R., McKenzie, D. (1989). Magmatism at rift zones: The generation of volcanic continental margins and flood basalts. Journal of Geophysical Research, 94, 7685-729.
Wilson, J.T. (1965). A new class of faults and their bearing on continental drift. Nature, 207, 343-347.